Paradoxical Loss of Excitation with High Intensity Pulses during Electric Field Stimulation of Single Cardiac Cells

Vinod Sharma, Robert C. Susil, and Leslie Tung
Department of Biomedical Engineering, The Johns Hopkins University, Baltimore, Maryland 21205

ABSTRACT Transmembrane potential responses of single cardiac cells stimulated at rest were studied with uniform rectangular field pulses having durations of 0.5–10 ms. Cells were enzymatically isolated from guinea pig ventricles, stained with voltage sensitive dye di-8-ANEPPS, and stimulated along their long axes. Fluorescence signals were recorded with spatial resolution of 17 μm for up to 11 sites along the cell. With 5 and 10 ms pulses, all cells ($n = 10$) fired an action potential over a broad range of field amplitudes (~3–65 V/cm). With 0.5 and 1 ms pulses, all cells ($n = 7$) fired an action potential for field amplitudes ranging from the threshold value (~4–8 V/cm) to 50–60 V/cm. However, when the field amplitude was further increased, five of seven cells failed to fire an action potential. We postulated that this paradoxical loss of excitation for higher amplitude field pulses is the result of nonuniform polarization of the cell membrane under conditions of electric field stimulation, and a counterbalancing interplay between sodium current and inwardly rectifying potassium current with increasing field strength. This hypothesis was verified using computer simulations of a field-stimulated guinea pig ventricular cell. In conclusion, we show that for stimulation with short-duration pulses, cells can be excited for fields ranging between a low amplitude excitation threshold and a high amplitude threshold above which the excitation is suppressed. These results can have implications for the mechanistic understanding of defibrillation outcome, especially in the setting of diseased myocardium.

INTRODUCTION

Electrical stimulation of the heart is commonly used therapeutically in the form of pacing, cardioversion, and defibrillation (Dell'Orfano and Naccarelli, 2001; Peters and Gold, 2001), yet the details of how cardiac tissue responds to applied currents and the accompanying extracellular fields are not fully understood. Toward the goal of gaining a more thorough understanding of electric field interactions with cardiac tissue, an isolated single cell has commonly been used as a model system (Cartee and Plonsey, 1992; Fishler et al., 1996; Gray et al., 2001; Heppner and Plonsey, 1970; Hund and Rudy, 2000; Knisley and Grant, 1995; Krassowska and Neu, 1994; Leon and Roberge, 1993; Linz et al., 1999; Meunier et al., 1999; Pumir et al., 1998; Ranjan et al., 1998; Tung et al., 1991; Windisch et al., 1995).

Cell excitation has been analyzed in one of two ways. The first is by current injection into the intracellular space (referred to as current injection; Gray et al., 2001; Hund and Rudy, 2000; Meunier et al., 1999; Pumir et al., 1998). Current injection results in a uniform polarization of the membrane if the cell length is short (compared with the space constant). Cell excitation occurs when the intracellular potential, and hence V_m, is raised above a threshold value for the regenerative activation of inward I_{Na}. Virtually all of the mechanistic concepts and terminology regarding the stimulation of excitable systems (such as the strength-duration relation, rheobase, voltage threshold, charge threshold, accommodation, and liminal length) have arisen from current injection models, including the work of Blair (1932), Fozzard and Schoenberg (1972), Jack et al. (1975), and Noble and Stein (1966).

In contrast, electrical stimulation of tissue rarely involves direct intracellular current injection, but rather, the flow of current from an extracellular stimulating electrode, which produces an electric field in the interstitial space (referred to as field stimulation; Cartee and Plonsey, 1992; Fishler et al., 1996; Knisley and Grant, 1995; Krassowska and Neu, 1994; Leon and Roberge, 1993; Meunier et al., 1999; Pumir et al., 1998; Stone et al., 1999; Susil et al., 1999; Tung and Borderies, 1992; Windisch et al., 1995). The electric field acts to polarize the cell membrane in a nonuniform fashion. This polarization pattern has been well characterized for an isolated cell system, the model system of choice in our study. When the field is aligned with the long axis of the cell, the largest polarization changes occur with opposite polarity at the ends of the cell (Cheng et al., 1999; Knisley and Grant, 1995), with a continuous change in polarization occurring along the cell length (Sharma and Tung, 1999; Windisch et al., 1995). Because of the nonuniform membrane polarization, ionic currents during field stimulation also have a spatially nonuniform profile. Thus, cell excitation during field stimulation occurs when the sum total of ionic currents along the

Submitted June 22, 2004, and accepted for publication November 23, 2004.

Address reprint requests to Dr. Leslie Tung, Dept. of Biomedical Engineering, The Johns Hopkins University, 720 Rutland Ave., Baltimore, MD 21205. Tel.: 410-955-7453; Fax: 410-955-0549; E-mail: ltung@bme.jhu.edu.

Vinod Sharma's present address is Medtronic Inc., Minneapolis, MN.

Abbreviations used: V_m, transmembrane potential; I_{Na}, transmembrane sodium current; I_{K1}, transmembrane inward rectifying potassium current; LLE, lower limit of excitation/lower field strength below which cell fails to excite; ULE, upper limit of excitation/upper field strength above which cell fails to excite.

0006-3495/05/04/3038/12 $2.00

doi: 10.1529/biophysj.104.047142

cell length produces a net inward current that raises the intracellular potential and average V_m of the cell above a threshold value (Tung and Borderies, 1992). Hence, like the case for current injection, field stimulation occurs in an all-or-none fashion once a threshold level is reached. However, it is important to keep in mind that the mechanistic basis for the stimulus threshold in terms of the flow of ionic currents is significantly different than that during current injection and is the focus of in-depth investigation of our study.

We hypothesize that the fundamental differences between stimulation by current injection and electric fields may become particularly evident at high field strengths and short pulse durations. Theoretical models based on current injection membranes predict that excitation will occur for currents of all strengths once a threshold is exceeded. This is because the injected current also brings in charge that further augments the intrinsic inward sodium current of the cell and depolarizes the membrane with increasing magnitude as the current amplitude increases. However, this situation does not apply to a nonuniformly polarized cell during field stimulation where there is no net injection of current into the cell and where the net depolarizing current arises solely from the intrinsic membrane currents. Not only is it possible that the net membrane current might not increase monotonically with the applied field strength, but the polarity of the current itself might not even remain inward at high field strengths.

In this study we sought to experimentally elucidate field-induced excitation of guinea pig ventricular cells, focusing particularly on high field strengths. To gain further insights into cellular excitation, we also performed computational studies using the Luo-Rudy phase 1 model (Luo and Rudy, 1991) of the guinea pig ventricular cell. These computational results provide a mechanistic understanding of our experimental results by unraveling the interplay between the ionic currents involved in the experimentally observed responses.

METHODS

Experiments were performed in enzymatically isolated guinea pig ventricular cells. The details of cell isolation and experimental setup have been described previously (Sharma and Tung, 2002). Briefly, guinea pigs (Hartley strain, weight 200–300 g) were sacrificed and their hearts extracted and perfused retrogradely via the aorta using a solution containing a mixture of protease and collagenase enzymes to dissociate cells. The cells were stained with 10–50 μM di-8-ANEPPS (Molecular Probes, Eugene, OR) for ~5 min and loaded into a chamber that could be rotated to allow alignment of the cell axis with the applied field. After waiting for 15–20 min, which allowed the majority of the cells to settle and affix to the bottom of the chamber, the cells were continuously perfused with normal Tyrode's solution maintained at 34°C–37°C. Tyrode's solution had the following composition (in mM): 135 NaCl, 5.4 KCl, 1 $MgCl_2$, 0.33 NaH_2PO_4, 5 HEPES, 1.8 $CaCl_2$, 5 glucose (adjusted to pH 7.4 with NaOH). The V_m responses of a cell were recorded by stimulating with a uniform electric field pulse (referred to as the S1 pulse) directed along its long axis and applied during the resting phase. Four different pulse durations were used: 0.5 ms, 1 ms, 5 ms, and 10 ms. In some experiments, the duration of the field pulse was kept constant while its amplitude was changed. In other experiments, the amplitude of the pulse was kept constant while the duration was changed. The actual field in the chamber was measured by recording the voltage drop across a pair of electrodes located in the chamber and oriented along the field direction. The fluorescence signals from the cell were recorded from up to 11 sites along the cell length using a multisite recording system (Sharma and Tung, 2002). Since dye-stained cells experience damage when exposed to intense excitation light (Schaffer et al., 1994), the recording duration for a single exposure was limited to ~50–100 ms. This allowed us to observe the responses to up to 15 S1 pulses of variable amplitude and duration in a single cell. The experiments were performed at a magnification of 60×, resulting in a resolution of 17 μm per site.

For the modeling portion of the study, a cell with 201 distinct patches and membrane kinetics as described by the phase 1 Luo-Rudy model (Luo and Rudy, 1991) was simulated using methods previously described (Susil et al., 1999; Tung and Borderies, 1992). The phase 1 Luo-Rudy model and its more advanced version, the phase 2 Luo-Rudy model (Luo and Rudy, 1994), are routinely used to study phenomena associated with defibrillation level fields (DeBruin and Krassowska, 1998; Rodriguez et al., 2004). An implicit assumption (and possible limitation) is that the various ionic currents in the two models that have been described over the physiological range of V_ms can be extrapolated to higher V_ms as are present during defibrillation level fields. The coupled differential equations were numerically solved for V_m of the various patches using the Crank-Nicholson integration method. The spatial discretization size was 0.6 μm, and a variable time step algorithm, limiting the maximum change in V_m to 50 μV, was used to control integration error. The model was coded in C and executed on a Dell Latitute, Pentium 4 computer running Windows XP (Dell, Round Rock, TX).

EXPERIMENTAL RESULTS

Cell excitation with longer duration (5 and 10 ms) field pulses

We have previously investigated V_m responses for fields applied during the early plateau of the action potential (Sharma and Tung, 2002). Here those findings have been extended to field stimulation applied during the resting phase. Cell excitation occurred at all field strengths tested (~3–65 V/cm) for 5 and 10 ms pulses ($n = 10$). A typical result for a 10 ms pulse of changing field strength is shown in Fig. 1. The V_m responses are shown superimposed for seven sites along the cell length. A common feature among the V_m responses for various field strengths was that in all cases V_m at the different sites immediately diverged from the resting potential with the onset of the field pulse, attained a state of maximal nonuniformity during the pulse, and then rapidly coalesced to a uniform plateau potential after the pulse break. However, the detailed dynamic behavior of V_m responses changed with increasing field strength. At 5 V/cm the cell fired an action potential after a slight delay from the make of the S1 pulse. With increasing field strengths, the delay decreased and became negligible at 28 V/cm. However, for a 41 V/cm pulse, the action potential occurred after the break of the S1 pulse. For a 56 V/cm pulse, the cell depolarized slowly throughout the duration of the S1 pulse although at a rate much slower than the normal action potential upstroke. After the pulse, the cell repolarized uniformly to the plateau potential.

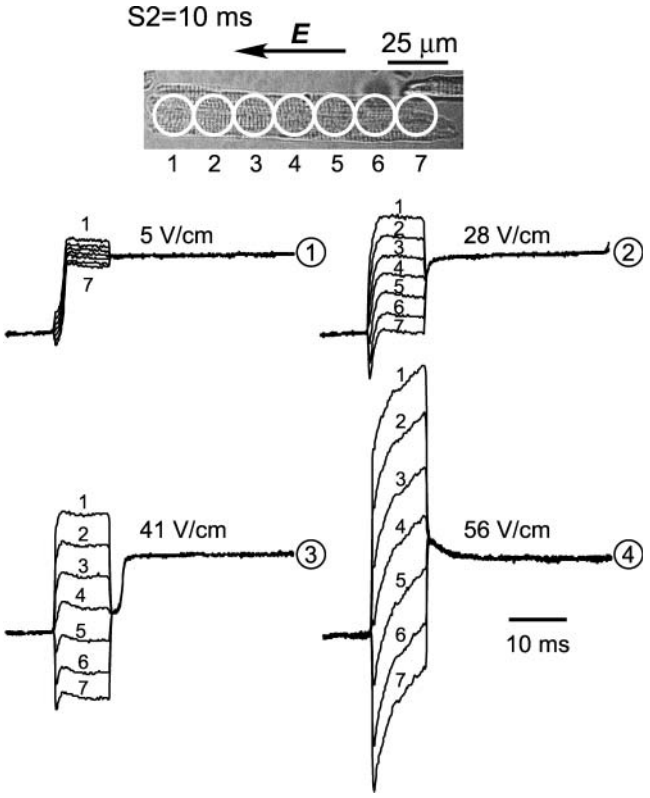

FIGURE 1 Cell excitation with 10 ms duration pulses. The cell shown was stimulated in the indicated direction with S1 pulse of 10 ms and variable amplitude, and V_m responses were optically recorded from seven sites spaced equally along the cell length. The four sets of recordings show V_m responses for the various S1 pulses. The numbers beneath and above the S1 portion of the recordings indicate the site number to which that trace corresponds. The amplitude of the S1 pulses is shown alongside the recordings. The circled numbers on the right of the traces indicate the sequence in which the recordings were obtained. The time bar for all recordings is shown alongside the 56 V/cm traces.

Paradoxical loss of excitation for shorter (0.5 and 1 ms) duration field pulses

Experiments were performed in $n = 7$ cells. As the field was gradually raised starting at a low level, all cells fired when the field reached a threshold value (~4–8 V/cm), referred to as the LLE. However, upon further increase in amplitude, five of seven cells could not be excited when field strength exceeded a higher threshold value, referred to as the ULE, that ranged between ~50 and 60 V/cm. An example of this result is shown in Fig. 2. The cell was stimulated with a series of 0.5 ms pulses of varying amplitude. It was excited with 44 and 60 V/cm pulses but not with a 64 V/cm pulse. To ensure that this loss of excitation was not merely the result of changes in the physiological state of the cell as a result of multiple exposures to the excitation light and to high field pulses, the field strength was lowered back to 60 V/cm and then to 43 V/cm. For both of these pulses, the cell responded by firing a normal action potential. Note that the field responses in Fig. 2 appear rounded because of the finite bandwidth (1.5 KHz) of our recording system. In actuality the rise time of V_m responses is in the microseconds range (Cartee and Plonsey, 1992; Hibino et al., 1993; Krassowska and Neu, 1994), and hence the responses in Fig. 2 and other figures showing data for short pulse experiments should mirror the rectangular morphology of the applied field pulses. Such is the case in the computer simulations.

The field-dependent transition from normal excitation to loss of excitation was not abrupt, but rather a gradual process as illustrated in Fig. 3. The cell shown in Fig. 3 was stimulated with a series of 1 ms pulses of increasing field strength. For field strengths of 36 and 48 V/cm, the cell fired an action potential either during or immediately after the S1 pulse. However, when the S1 amplitude was increased to 53 V/cm, the cell fired after a considerable delay (~6 ms) from the S1 make. Finally, when the S1 amplitude was increased to 60 V/cm the cell excitation was completely suppressed. Again, the normalcy of cell state was ascertained by ensuring that the cell was excitable for a lower strength field pulse (data not shown).

We investigated the relationship between paradoxical loss of excitation and pulse duration by performing experiments in which ULE was first determined for a 0.5 ms pulse and then the pulse duration was gradually increased. Fig. 4 shows the result of one such experiment. ULE was between 50 and 55 V/cm as the cell was excited with a 50 V/cm pulse but failed to excite with a 55 V/cm pulse (Fig. 4, *upper box*). With field strength held constant at 55 V/cm, the pulse duration was incrementally increased to 1, 5, and 10 ms (Fig. 4, *lower box*). Although the cell remained unexcited for the 1 ms pulse, a normal action potential was elicited for 5 and 10 ms pulses.

The data for all seven cells and a total of 81 field stimuli are summarized in Fig. 5. To account for the differences in cell length, we scaled the field by a factor of $L/120$, where L is the length of a given cell in micrometers. This scaled field is the effective field experienced by a 120 μm long cell, which is the average length of a guinea pig cardiac cell (Watanabe et al., 1985). The mean ($\pm$SD) LLE in terms of scaled field for the seven cells was found to be 8.2 $\pm$ 2.8 V/cm. The mean ULE for five cells in which the excitation was suppressed upon reaching an upper threshold was 57.8 $\pm$ 5.6 V/cm (range = 50.8–60.7 V/cm at a confidence level of 95%). Possible reasons for the lack of paradoxical unexcitation in two of the cells will be discussed in the Discussion section.

COMPUTATIONAL RESULTS

Paradoxical loss of excitation with shorter duration field pulses

A model cell with Luo-Rudy phase 1 membrane dynamics was stimulated with 1 ms pulses at ~6.27 V/cm and at ~59 V/cm (Fig. 5). Note that although the simulations were performed using a 201-patch model cell, for clarity, traces

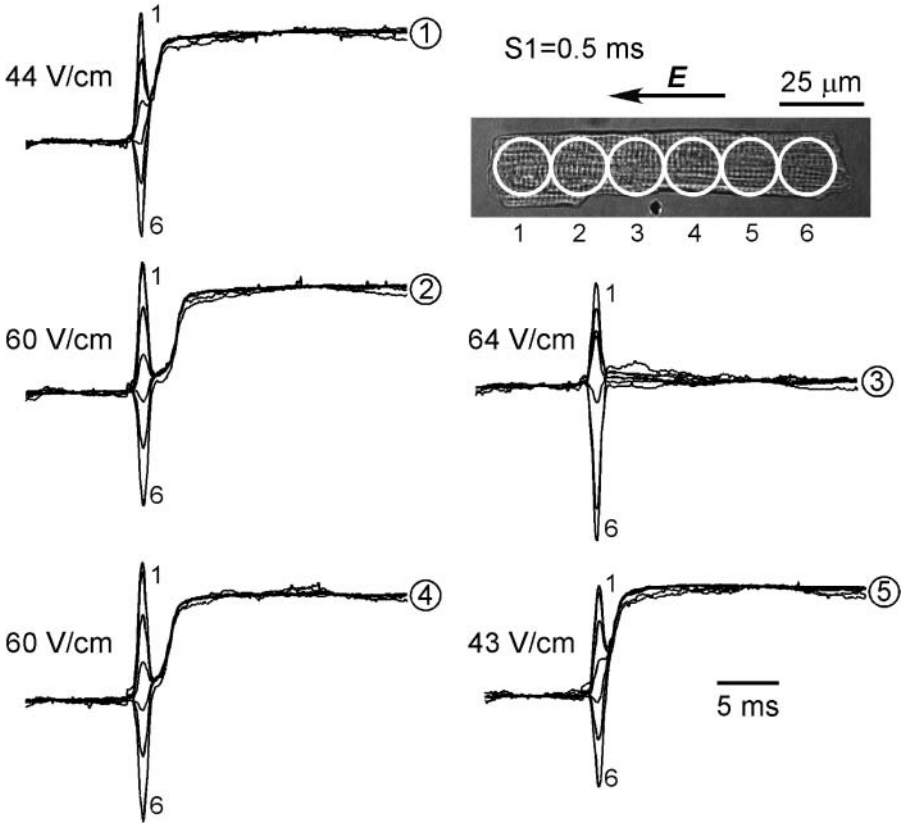

FIGURE 2 Loss of excitation for 0.5 ms pulses. The cell shown was stimulated with a series of 0.5 ms pulses of variable amplitude. The cell could be excited with 44 and 60 V/cm pulses but not with the 64 V/cm pulse. Excitation was restored when field strength was decreased back to 60 and 43 V/cm. The circled numbers on the right of the traces indicate the sequence in which the S1 pulses were applied. Also indicated are the recordings corresponding to sites 1 and 6. The time bar shown for the 43 V/cm recordings is common to all five sets of traces.

are shown for 11 sample patches only. Furthermore, in Figs. 6–9 and the text that follows, patch 1 is referred to as patch 1, patch 21 as patch 2, patch 41 as patch 3, and so forth, to where patch 201 is referred to as patch 11. The V_m responses from the central patch (equivalent to the average V_m of the cell; Sharma et al., 2002) are shown in Fig. 6. For pulses at ~6.27 V/cm, V_m from all patches showed a depolarizing trend during the S1 pulse for all amplitudes, followed by an action potential after the S1 break. However, the cell transitioned from an unexcited to excited state as field strength was increased from 6.26 V/cm to 6.28 V/cm (LLE = 6.28 V/cm), whereas it transitioned back to the unexcited state as field strength was increased from 58 V/cm to 60 V/cm (ULE = 58 V/cm).

Fig. 7 shows the time course of sodium current (I_{Na}) and inwardly rectifying K^+ current (I_{K1}) for fields near LLE (~6.3 V/cm), directly beneath their respective V_m traces for the 11 equally spaced patches taken across the length of the model cell. During the S1 pulse, an inward spike of I_{Na} was observed in the four leftmost patches (patches 1–4). I_{Na} was largest (600 $\mu A/cm^2$) in the maximally depolarized patch 1. It gradually declined and became negligible as V_m transitioned to hyperpolarized potentials in the opposite regions of the cell (patches 7–11). After the break of the S1 pulse, a second spike in I_{Na} was observed, but this was largest (408 $\mu A/cm^2$) at the cell end that was maximally hyperpolarized during the S1 pulse (patch 11) and gradually declined, moving toward the depolarized end of the cell (I_{Na} for patch 1 = 230 $\mu A/cm^2$).

The spatial pattern of I_{K1} amplitude was qualitatively opposite to what was observed for I_{Na} except that, unlike I_{Na}, no current spike was observed after the S1 break. At the onset of the field pulse, an instantaneous change in I_{K1} occurred in all membrane patches except in the central patch (patch 6). The initial change in I_{K1} at the S1 onset was inward and largest (20 $\mu A/cm^2$) at the maximally hyperpolarized end of the cell that faced the anode (patch 11), declined gradually to zero moving from patch 11 to 6, and was outward but low in amplitude for patches 1–5 ($I_{K1} = 2.5$ $\mu A/cm^2$ for patch 1). After the initial change in I_{K1}, a positive trend (i.e., decrease in inward current and eventual reversal to outward current in some patches) was observed later during the S1 pulse for patches 7–11, and a slight negative trend (i.e., decrease in outward current) was observed for patches 1–5. Thus, the I_{K1}s of the two halves of the cell crisscrossed each other during the latter half of the S1 pulse. After the break of the pulse, I_{K1} was slightly positive (i.e., a small net outward current) and of uniform value along the cell length because V_m converged to a single level positive to the prepulse resting potential. However, when the cell fired, I_{K1} decreased and became negligible during the plateau of the action potential.

The patterns of V_m, I_{Na}, and I_{K1} for fields near ULE are depicted in Fig. 8. For both field strengths of 58 and 59 V/cm,

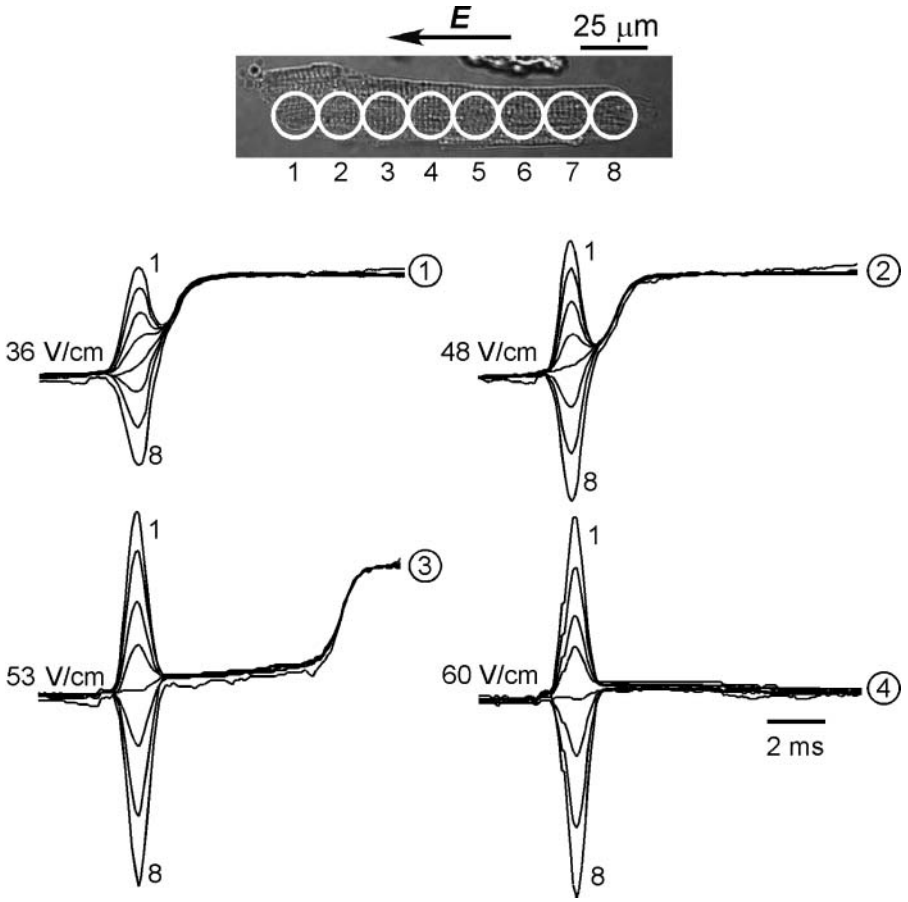

FIGURE 3 Delay and loss of excitation for 1 ms pulses. The cell shown was stimulated with a series of S1 pulses of increasing amplitude. The cell fired normally for 36 and 48 V/cm pulses. For the 53 V/cm pulse, a delay of ~6 ms (measured from the S1 break) was observed before cell excitation occurred. For the 60 V/cm pulse, the cell failed to fire an action potential. The circled numbers on the right of the traces indicate the sequence in which the recordings were obtained. Also numbered in each set of traces are responses corresponding to sites 1 and 8. The time bar for the 60 V/cm recordings is common to all sets of recordings.

V_m showed similar depolarizing trends, and I_{Na} and I_{K1} were also similar during the pulse. In contrast to the I_{Na} behavior for a near LLE pulse that was inward or zero in all the patches during the field pulse (Fig. 7), I_{Na} for a field pulse near ULE was outward for patches 1, 2, and 3, which experienced extremely large levels of depolarization. Patches 4 and 5 were the only two that exhibited inward current, with patch 5 showing a peak in current later during the pulse. Patches 6–11 from the hyperpolarized half of the cell had negligible I_{Na}. I_{K1} was negative and large in the hyperpolarized patches (7–11) and negligible in the depolarized patches (1–5). Together, the currents summed to a net inward current that acted to depolarize the average V_m of the cell. The key difference in the responses to the two fields is that for the 58 V/cm pulse, the cell was uniformly polarized at −55 mV after the pulse break and persisted at this level for ~2 ms, after which the cell fired an action potential. In contrast, the postpulse V_m for the 59 V/cm field was slightly more negative at −57 mV, and consequently, the cell failed to fire.

Return of excitation with longer duration pulses

Fig. 9 depicts the return of cell excitation as the pulse duration was gradually increased from 1 ms for a supra-ULE (59 V/cm) pulse for which the cell failed to excite. At a 2 ms pulse duration, the cell fired an action potential, and the initial plateau potential at the pulse break was +27 mV, a level slightly more positive than the +25 mV attained upon excitation with a shorter duration, near-ULE level pulse (see response to 1 ms, 58 V/cm pulse in Fig. 6 *C*). I_{K1} exhibited a behavior similar to that for the 1 ms pulse except that now the current was present for a longer duration. The continued presence of inward current enabled V_m at all patches to depolarize to levels not attained with the 1 ms pulse. Consequently, the behavior of I_{Na} for the 2 ms pulse was more complex than that for the 1 ms pulse. During the latter part of the pulse, a rush of inward I_{Na} occurred in patch 6 of the cell, a patch that was hyperpolarized earlier during the pulse but later depolarized gradually up to the activation threshold for I_{Na}. After the pulse break, a rush of inward I_{Na} occurred synchronously in patches 7–11, the regions of the cell that remained hyperpolarized during the field pulse but became depolarized to above the I_{Na} activation threshold after the pulse.

For the 4 ms pulse, the dynamics of I_{Na} and I_{K1} during the first half were identical to those for the 2 ms pulse. However, in the latter half, a second spike of inward current coming from patch 7 was observed, a consequence of the continuing

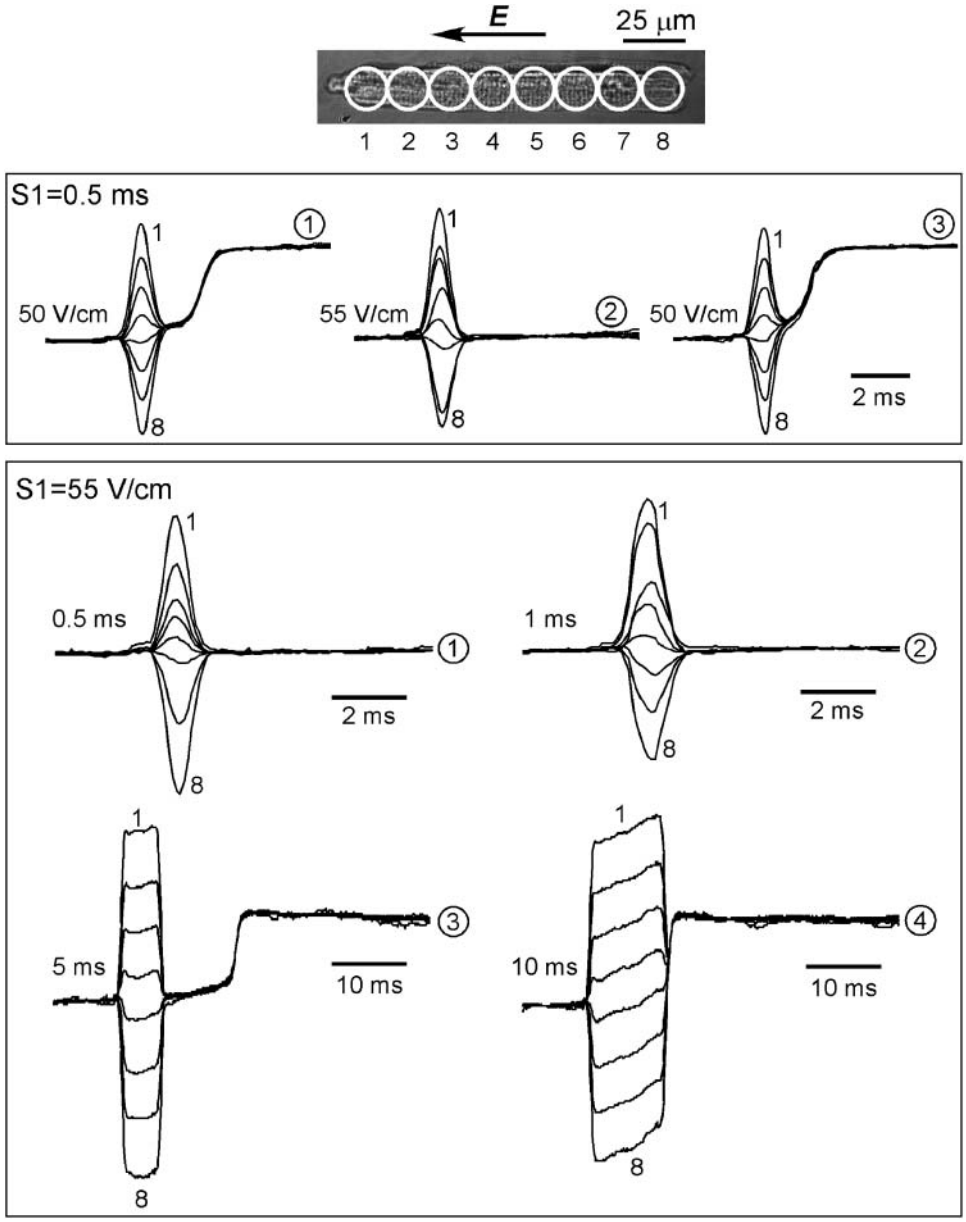

FIGURE 4 Return of excitation with increase in pulse duration. (*Upper box*) The cell shown was stimulated successively with three S1 pulses of 50, 55, and 50 V/cm. The cell was excited with the 50 V/cm pulses, but not with the 55 V/cm pulse. The time bar on the right applies to all three sets of recordings. (*Lower box*) With S1 amplitude fixed at 55 V/cm, the S1 amplitude was increased from 0.5 ms to 1 ms, 5 ms, and 10 ms. The cell did not fire an action potential for the 0.5 ms and 1 ms pulses but fired for the 5 ms and 10 ms pulses. Note the delay in excitation for the 5 ms pulse. The circled numbers indicate sequence of stimulation. The recordings corresponding to sites 1 and 8 have also been numbered in each set of traces.

depolarizing trend of the cell during the pulse. After the pulse terminated, the cell was polarized to a uniform potential of +62 mV brought about by the longer duration of I_{K1} currents. This was accompanied by a spike of outward I_{Na} in patches 8–11 that were the most hyperpolarized during the field pulse.

DISCUSSION

In this study, we used a combination of experimental and computational approaches to investigate the behavior of guinea pig ventricular cell excitation with short-duration field stimuli. The main results of the study are as follows:

1. For a field pulse that is 1 ms or shorter in duration, the cardiac cells can be excited for fields ranging between a lower threshold of ~4–8 V/cm (5–12 V/cm scaled field; LLE) and a higher field threshold of ~50–60 V/cm (52–64 V/cm scaled field; ULE). Outside of this field range the cells cannot be excited.
2. I_{K1} and I_{Na} are the two main currents that are present during field stimulation at rest, and according to computer simulations, the interplay between them causes a paradoxical loss of excitation for fields above ULE. Whereas I_{K1} is primarily inward along the cell length for all field strengths, I_{Na} is inward at low field strengths and becomes predominantly outward during the field pulse at high field strengths.
3. Starting at a short duration and high amplitude field pulse above ULE for which paradoxical loss of excitation is observed, the cell can be excited as the pulse duration is

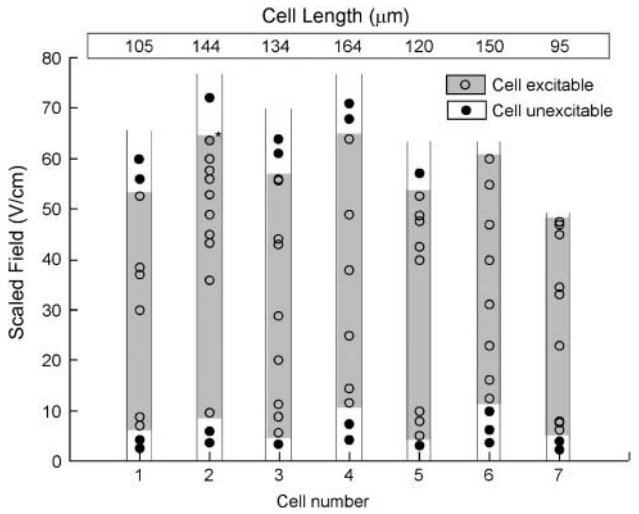

FIGURE 5 Summary of data for seven cells stimulated with short (0.5 and 1 ms) pulses. The zone of excitation and lack thereof for each of the seven cells is shown individually. Each circle represents an applied field stimulus. Open circles represent the field stimuli for which excitation occurred, and solid circles represent the fields for which a cell failed to excite. For cell 2, the data point with an asterisk represents the stimulus corresponding to trace 3 of Fig. 3 for which excitation occurred after a considerable delay from the stimulus pulse. Note that the ordinate is the scaled electric field and represents an equivalent field experienced by a 120-μm long cell, which is the nominal length of a guinea pig cell. Cell lengths for various cells are shown at the top of the plot.

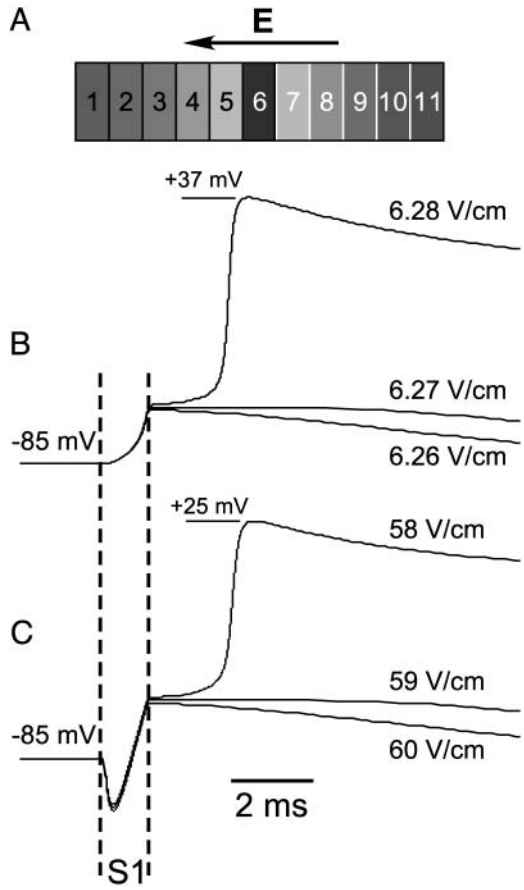

FIGURE 6 Responses of a model cell for 1 ms pulses near the LLE and near the ULE. Panel *A* shows the schematic of the model cell divided into 201 equal sized patches, but for simplicity only 11 (every one in 20 patches) are shown. Panel *B* shows the response of the central patch to three low amplitude pulses near LLE. Panel *C* shows the superimposed responses from the same patch for three pulses near ULE. The cell was excited with 58 V/cm but not with 59 and 60 V/cm pulses. The takeoff potential for 6.28 and 58 V/cm pulses is the same (~ -55 mV) and is equal to the Na^+ channel activation threshold. However, the overshoot potentials are different (+37 and +25 mV, respectively).

increased. I_{K1} plays a key role in this transition. It is large and inward in the anode-facing hyperpolarized regions of the cell, diminishes toward the center of the cell, and becomes outward but is relatively small in the depolarized regions of the cell. In contrast, I_{Na} is predominantly outward in the depolarized regions of the cell immediately after the pulse onset. However, after some delay, a spike of inward current is observed in the central region of the cell that sweeps across the membrane toward the anode-facing hyperpolarized end of the cell (Fig. 9). This inward I_{Na} together with the continuing presence of inward I_{K1} as pulse duration is increased depolarizes the average V_m of the cell to a level positive to the activation threshold of I_{Na}, so that upon the break of the pulse, I_{Na} is triggered in the patches of cell membrane that were hyperpolarized during the field pulse.

A cell stimulated by current injection undergoes uniform polarization across its length and has spatially uniform membrane dynamics provided that its length is much shorter than a space constant. In contrast, during field stimulation various regions of the cell experience very different V_ms and therefore can exhibit starkly different membrane dynamics. Irrespective of the method of stimulation (field stimulation or current injection), a cell is considered to be excited when there is a net inward current that elevates its V_m to the plateau level. During current injection, this is accomplished when the membrane potential of the space clamped cell reaches the threshold for regenerative opening of Na^+ channels, resulting in a large inward current. However, inward current is also provided by the stimulus current so that it is still possible to excite the cell even in the absence of I_{Na} if higher stimulus strengths are used. In contrast, in a field-stimulated and nonuniformly polarized cell, there is no net contribution of the stimulus current to changes in the cellular V_m. Instead, the changes are caused solely by the intrinsic membrane currents, which can vary in amplitude and direction (i.e., inward versus outward) in different regions along the cell length. The summation of these currents can result in either a net inward current that produces global depolarization or a net outward current that produces global hyperpolarization of the cell. This global polarization, which can be characterized as the component

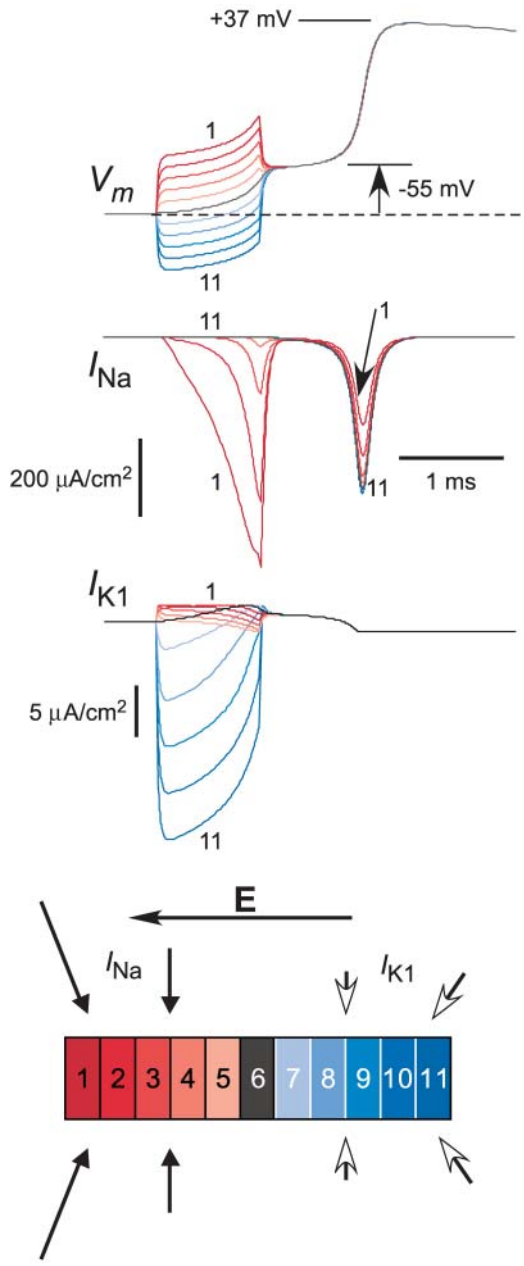

FIGURE 7 V_m response and ionic currents (I_{Na} and I_{K1}) of a model cell stimulated with a field pulse at LLE. The model cell of Fig. 6 *A* was stimulated with a 5 ms field pulse of ~6.3 V/cm in the indicated direction. The V_m responses from the 11 representative patches are shown in the topmost set of traces, and I_{Na} and I_{K1} from the various patches are shown in the traces directly below. The numbers adjacent to the three sets of traces indicate the patch number to which that recording corresponds. For clarity, only traces from the end patches have been numbered. At the bottom is a schematic cell that shows the flow of I_{Na} and I_{K1} in the various patches. The various arrows signify the relative amplitudes of the corresponding currents.

of the response that is common to all patches along the cell length (Sharma et al., 2002), manifests itself as parallel time courses of responses in the different regions of the cell (see Fig. 1).

The key to understanding the paradoxical loss of excitation for fields higher than ULE lies in the behavior of I_{K1} and I_{Na} with increasing field strength. The current-voltage (I-V) relationship of I_{K1} is inwardly rectifying and exhibits a large inward current for potentials negative to ~−85 mV (Hume and Uehara, 1985). For potentials positive to this value, I_{K1} is outward and small. Thus, for fields near both LLE and ULE, a large inward I_{K1} is activated in the hyperpolarized regions of the cell (Figs. 7–9) that acts to depolarize the cell. However, as the net inward current brought in via I_{K1} depolarizes each of the membrane patches during the pulse (upward trend in V_m in Figs. 7–9), the driving force for I_{K1} decreases in the hyperpolarized regions, and I_{K1} slowly declines. Furthermore, for a given cell patch in the anodal region of the cell, the peak of inward I_{K1} occurs immediately after the pulse onset and increases monotonically in amplitude with the field strength.

The behavior of I_{Na} is more complicated and results from its voltage- and time-dependent kinetic properties. Starting at the make of the field pulse, the depolarization in the cathode-facing half of the cell leads to a rapid activation and inactivation of the Na^+ channels and a spike of I_{Na}. The polarity of the current spike, however, depends on the strength of the applied field. At low field strengths near LLE, for which the maximally depolarized end of the cell remains negative to the Na^+ channel reversal potential of ~+55 mV (Nilius, 1988), the driving force for the sodium ions is inward (Fig. 7). However, as the field strength is increased to near ULE, the maximum depolarization is elevated positive to the reversal potential of the Na^+ channels, and I_{Na} becomes outward (Fig. 8). Thus, for fields near LLE both I_{Na} and I_{K1} are inward and work synergistically to depolarize the cell (Tung and Borderies, 1992). However, for fields near ULE the initial outward spike of I_{Na} acts to hyperpolarize the cell and opposes the depolarizing effect of I_{K1}. Consequently, for short-duration and high amplitude pulses above ULE the net inward current during the pulse is negligible or small and inadequate to raise the average V_m of the cell to the Na^+ channel threshold at the pulse break, leading to the paradoxical loss of excitation. Our experimental data showing the immediate recovery of cell excitation upon reduction in field strength (Figs. 2 and 4) support an opposing interplay between I_{Na} and I_{K1} as the major mechanism for this loss of excitation and argue against any irreversible loss of cell excitability via processes such as electroporation (Tung, 1995).

For longer pulse durations, a component of I_{Na} may be present at the pulse break and always occurs in regions of the cell that were hyperpolarized and remained negative to the threshold for Na^+ channel activation during the field pulse (Figs. 8 and 9). When the stimulus terminates and the cell returns to a uniform potential, these hyperpolarized regions are primed to activate I_{Na} and result in an inward current if the poststimulus potential is positive to the activation threshold for I_{Na} and negative to its reversal potential. This postpulse component of I_{Na} can also be outward if the postpulse

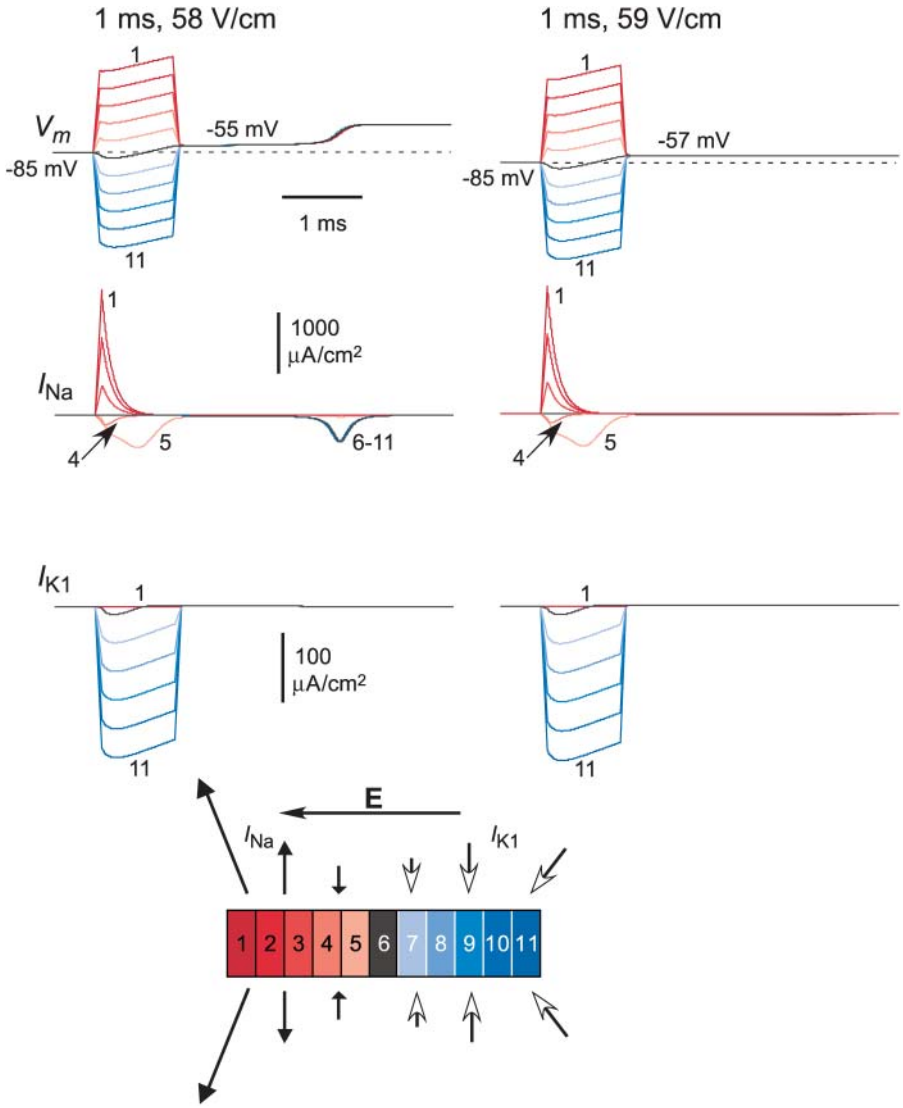

FIGURE 8 Paradoxical loss of excitation in a model cell for fields near ULE. The left column shows V_m, I_{Na}, and I_{K1} for the 11 patches of the model cell for a 58 V/cm, 1 ms field pulse. The right column shows V_m, I_{Na}, and I_{K1} for a pulse also of 1 ms duration but with amplitude increased to 59 V/cm. The numbers indicate the patch numbers to which various traces correspond. For clarity, only traces from the end patches are numbered for V_m and I_{K1}. For I_{Na}, intermediate patches with complex temporal behavior are also indicated. Time bar is applicable to all sets of traces. I_{Na} and I_{K1} amplitude bars are applicable to both 58 and 59 V/cm traces. At the bottom is a schematic cell that shows the flow of I_{Na} and I_{K1} in the various patches. The various arrows signify the relative amplitudes of the corresponding currents. The simulations in this figure are the same as in Fig. 6 *C*.

potential is positive to the reversal potential of I_{Na} (Fig. 9, 4 ms pulse). Additional components of I_{Na} can be present during the field pulse, especially with longer duration pulses (e.g., 2 and 4 ms pulses in Fig. 9). These arise with the sequential depolarization of the various patches as they are raised up to the Na^+ channel threshold. Note that the apparently saltatory behavior of I_{Na} depicted in Fig. 9 is a result of the fact that only 11 sample patches are depicted, and in reality the activation of Na^+ channels would be a smooth process as depolarization sweeps along the cell length toward the anodal-facing hyperpolarized end of the cell.

We found that the magnitude of the ULE is variable, ranging from 52 to 64 V/cm in five cells (Fig. 5). An explanation for this finding comes from our computer simulations (Fig. 10), which show that the ULE will vary, depending on the amount of I_{Na} and I_{K1} in the cell. The distribution of I_{Na} and I_{K1} is not homogeneous in the ventricles. I_{Na} is larger in the endocardial cells than in the epicardial cells by ~50% (Ashamalla et al., 2001). For I_{K1} this gradient is reversed, and it is larger in the epicardial cells than in the endocardial cells by ~13% (Liu et al., 1993). Thus, epicardial cells have less I_{Na} and more I_{K1}, two conditions that our simulation studies show will increase ULE. We have also found that variability in I_{Na} and I_{K1} also causes variation in the LLE, in a manner that roughly mirrors the variation in ULE (simulations not shown). Paradoxical unexcitation was not observed in two cells (cells 6 and 7, Fig. 5). The simplest explanation is that the maximum fields that were applied to those cells were not high enough to exceed their ULEs. Based on the LLEs, one might expect the ULE of cell 6 to be roughly that of cell 4, and the ULE of cell 7 to be roughly that of cell 3. In both cases, the expected ULEs were higher than the maximum fields that were applied.

During field stimulation, a polarization response of the tissue can occur far from the electrodes as a result of intracellular discontinuities (e.g., gap junctional resistances,

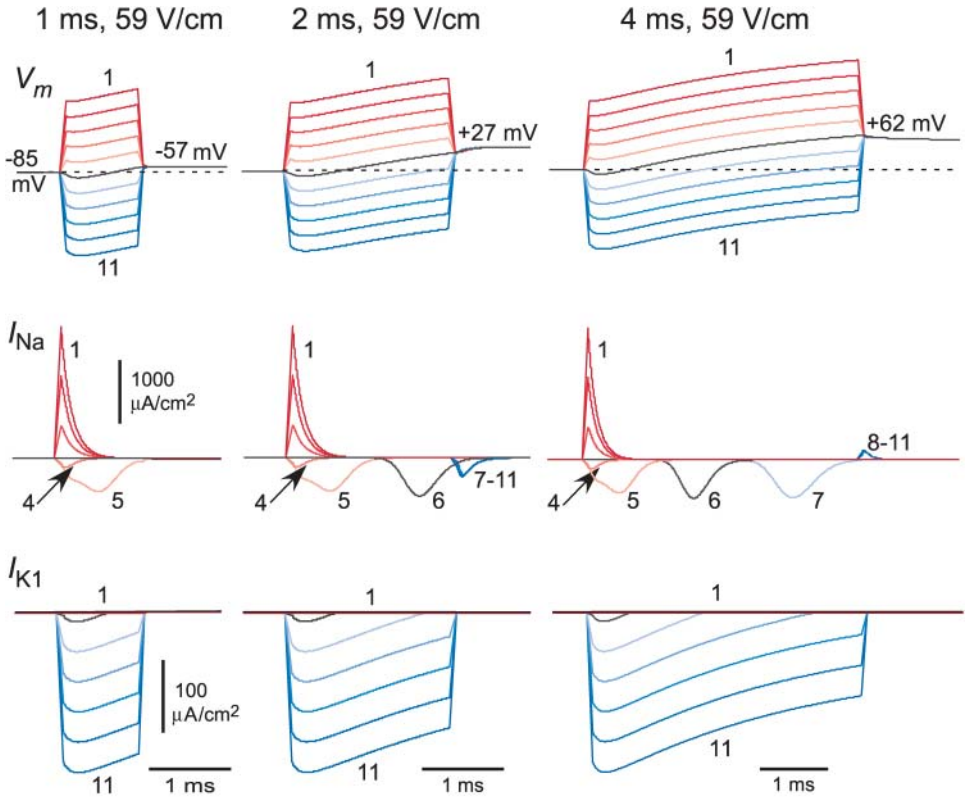

FIGURE 9 Return of excitation with increasing pulse duration. Left, middle, and right columns show V_m, I_{Na}, and I_{K1} for three pulses of equal amplitude (59 V/cm) but increasing duration (1, 2, and 4 ms, respectively). The cell was unexcited for a pulse duration of 1 ms but excited with 2 and 4 ms pulses. For clarity, only traces from the end patches are numbered for V_m and I_{K1}. For I_{Na}, intermediate patches with complex temporal behavior are also numbered. Time bar in each column is applicable to all sets of traces at that duration. I_{Na} and I_{K1} amplitude bars are applicable to all three durations.

cleft spaces, bundle and sheet structures). These discontinuities generate paired virtual sources of opposite polarity that produce adjacent regions of opposite polarization in the tissue (Sobie et al., 1997), akin to the oppositely polarized ends of the field-stimulated single cell. As the separation between the virtual sources increases, the magnitudes of polarization rise and level off when the separation reaches a value significantly (e.g., 3×) larger than the space constant, which is of the order of 1 mm (Susil et al., 1999). At the same time, there is less interaction between the two regions of opposite polarity and in the limiting case where the distances between the virtual sources is infinite, the oppositely polarized responses are independent of one another. Thus, the length scale of tissue discontinuities will presumably govern the range of field intensities for which paradoxical loss of excitation may be observed in tissue. Recently, microscopic measurements from transmural wedge preparations of the pig heart have shown that regions of opposite polarity occur over a length scale of the order of 0.5 mm (Sharifov et al., 2004).

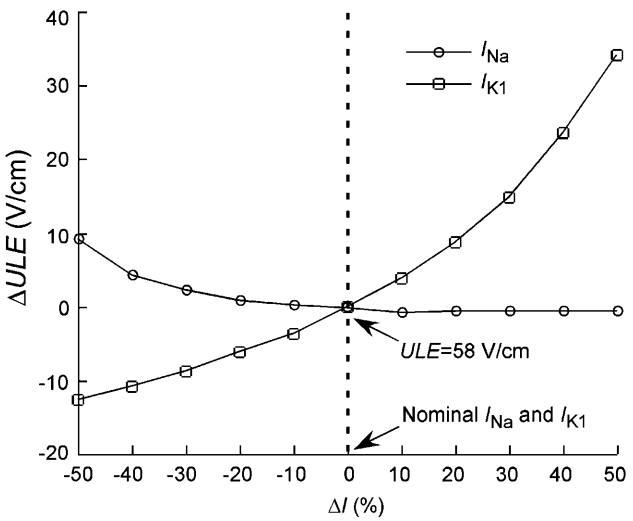

FIGURE 10 Change in ULE (ΔULE) of a model cell with varying I_{Na} and I_{K1} (ΔI). The I_{Na} and I_{K1} in the model cell of Fig. 6 *A* were varied and ULE determined by gradually increasing the amplitude of a 1 ms field pulse. The ordinate shows ΔULE compared to that of a cell having nominal I_{Na} and I_{K1}.

In addition to providing fundamental insights into field stimulation of cardiac cells and tissue, our observations may also have implications for the strong electrical shocks used to treat cardiac arrhythmias. As described earlier, tissue discontinuities arising from intercellular gap junctions, fiber bundles and sheet structures may give rise to microscopic regions of opposite polarity, an effect referred to as the ''sawtooth'' response in the cardiac literature. However, in healthy, well-coupled tissue the magnitude of the responses will be much smaller than those observed in the isolated single cell, so that paradoxical loss of excitation is unlikely to occur even with defibrillation level shocks. Our previously

published finding that the sawtooth effect arising from intercellular gap junctions is relatively small in isolated cell-pairs supports this notion (Sharma and Tung, 2001).

However, after a severe myocardial infarction, as is the case for the majority of the implantable cardioverter defibrillator patients (Anderson et al., 1999; Connolly et al., 2000), a thin layer of tissue that is only a few cells thick survives as an endocardial or epicardial border zone that abuts a necrotic core consisting of inexcitable fibroblasts (Jugdutt, 2003). Furthermore, the intercellular coupling in the border zone layer can be reduced by an order of magnitude (Yao et al., 2003) as gap junctions in this region undergo significant disruption (Matsushita et al., 1999; Peters et al., 1997). Such conditions are ideal for generating a large sawtooth effect at a length scale that is compatible with a paradoxical loss of excitation at high field strengths as are used during defibrillation. As a consequence, the tissue can be left in a heterogeneous state of excitation after the shock, a setting conducive for postshock slow propagation leading to shock failure. Indeed, several studies have noted that defibrillation efficacy first increases with an increase in field strength but then decreases with further increase in shock intensity (Fotuhi et al., 1999; Jones and Jones, 1980). Electroporation mediated damage to the cell membranes could be one of the mechanisms for this effect (Tung, 1996). We suggest that paradoxical loss of excitation at higher field strengths could be another important factor underlying the loss of defibrillation efficacy, particularly for short-duration pulses.

A possible limitation of our results is that the Luo-Rudy model that was used in the numerical simulations may not be applicable outside the physiological range of V_ms that may be present during defibrillation level fields. To address this possibility, we performed additional simulations in which two additional currents, a hypothetical outward current (I_a) and an electroporation current (I_{ep}) that may be present with large V_ms (Cheng et al., 1999), were added to the phase 1 Luo-Rudy model (not shown). Under these conditions, we found that the phenomenon of the ULE is still present, although its threshold is somewhat lower (primarily because of I_a), and the roles of I_{Na} and I_{K1} are blunted. We chose not to include these currents in our study because they have not been well characterized, and in the case of I_a the current's existence has not yet been confirmed experimentally. Nevertheless, with I_a and I_{ep} included, the analysis of the interplay of outward and inward currents is expected to get more complex.

In conclusion, we have shown that for excitable biological systems such as the cardiac cell, the notion of 'more is better' for the purposes of excitation may not always hold. The combination of electrophysiological characteristics that can render an excitable system susceptible to paradoxical loss of excitation at high field strengths are 1), that the system has a mix of ionic currents with nonlinear current-voltage relationships and opposite reversal potentials, and 2), that the system is strongly polarized in a nonuniform fashion over a length scale small enough that opposing excitatory responses interact.

REFERENCES

Anderson, J. L., A. P. Hallstrom, A. E. Epstein, S. L. Pinski, Y. Rosenberg, M. O. Nora, D. Chilson, D. S. Cannom, and R. Moore. 1999. Design and results of the antiarrhythmics vs implantable defibrillators (AVID) registry. The AVID investigators. *Circulation.* 99:1692–1699.

Ashamalla, S. M., D. Navarro, and C. A. Ward. 2001. Gradient of sodium current across the left ventricular wall of adult rat hearts. *J. Physiol.* 536:439–443.

Blair, H. A. 1932. On the intensity-time relations for stimulation by electric currents. II. *J. Gen. Physiol.* 15:731–755.

Cartee, L. A., and R. Plonsey. 1992. The transient subthreshold response of spherical and cylindrical cell models to extracellular stimulation. *IEEE Trans. Biomed. Eng.* 39:76–85.

Cheng, D. K., L. Tung, and E. A. Sobie. 1999. Nonuniform responses of transmembrane potential during electric field stimulation of single cardiac cells. *Am. J. Physiol.* 277:H351–H362.

Connolly, S. J., M. Gent, R. S. Roberts, P. Dorian, D. Roy, R. S. Sheldon, L. B. Mitchell, M. S. Green, G. J. Klein, and B. O'Brien. 2000. Canadian implantable defibrillator study (CIDS): a randomized trial of the implantable cardioverter defibrillator against amiodarone. *Circulation.* 101:1297–1302.

DeBruin, K. A., and W. Krassowska. 1998. Electroporation and shock-induced transmembrane potential in a cardiac fiber during defibrillation strength shocks. *Ann. Biomed. Eng.* 26:584–596.

Dell'Orfano, J. T., and G. V. Naccarelli. 2001. Update on external cardioversion and defibrillation. *Curr. Opin. Cardiol.* 16:54–57.

Fishler, M. G., E. A. Sobie, N. V. Thakor, and L. Tung. 1996. Mechanisms of cardiac cell excitation with premature monophasic and biphasic field stimuli: a model study. *Biophys. J.* 70:1347–1362.

Fotuhi, P. C., A. E. Epstein, and R. E. Ideker. 1999. Energy levels for defibrillation: what is of real clinical importance? *Am. J. Cardiol.* 83:24D–33D.

Fozzard, H. A., and M. Schoenberg. 1972. Strength-duration curves in cardiac Purkinje fibres: effects of liminal length and charge distribution. *J. Physiol.* 226:593–618.

Gray, R. A., D. J. Huelsing, F. Aguel, and N. A. Trayanova. 2001. Effect of strength and timing of transmembrane current pulses on isolated ventricular myocytes. *J. Cardiovasc. Electrophysiol.* 12:1129–1137.

Heppner, D. B., and R. Plonsey. 1970. Simulation of electrical interaction of cardiac cells. *Biophys. J.* 10:1057–1075.

Hibino, M., H. Itoh, and K. Kinosita Jr. 1993. Time courses of cell electroporation as revealed by submicrosecond imaging of transmembrane potential. *Biophys. J.* 64:1789–1800.

Hume, J. R., and A. Uehara. 1985. Ionic basis of the different action potential configurations of single guinea-pig atrial and ventricular myocytes. *J. Physiol.* 368:525–544.

Hund, T. J., and Y. Rudy. 2000. Determinants of excitability in cardiac myocytes: mechanistic investigation of memory effect. *Biophys. J.* 79: 3095–3104.

Jack, J. J. B., D. Noble, and R. W. Tsien. 1975. Electric Current Flow in Excitable Cells. Clarendon Press, Oxford.

Jones, J. L., and R. E. Jones. 1980. Postshock arrhythmias—a possible cause of unsuccessful defibrillation. *Crit. Care Med.* 8:167–171.

Jugdutt, B. I. 2003. Ventricular remodeling after infarction and the extracellular collagen matrix: when is enough enough? *Circulation.* 108:1395–1403.

Knisley, S. B., and A. O. Grant. 1995. Asymmetrical electrically induced injury of rabbit ventricular myocytes. *J. Mol. Cell. Cardiol.* 27:1111–1122.

Krassowska, W., and J. C. Neu. 1994. Response of a single cell to an external electric field. *Biophys. J.* 66:1768–1776.

Leon, L. J., and F. A. Roberge. 1993. A model study of extracellular stimulation of cardiac cells. *IEEE Trans. Biomed. Eng.* 40:1307–1319.

Linz, K. W., C. von Westphalen, J. Streckert, V. Hansen, and R. Meyer. 1999. Membrane potential and currents of isolated heart muscle cells exposed to pulsed radio frequency fields. *Bioelectromagnetics.* 20:497–511.

Liu, D. W., G. A. Gintant, and C. Antzelevitch. 1993. Ionic bases for electrophysiological distinctions among epicardial, midmyocardial, and endocardial myocytes from the free wall of the canine left ventricle. *Circ. Res.* 72:671–687.

Luo, C. H., and Y. Rudy. 1991. A model of the ventricular cardiac action potential. Depolarization, repolarization, and their interaction. *Circ. Res.* 68:1501–1526.

Luo, C. H., and Y. Rudy. 1994. A dynamic model of the cardiac ventricular action potential. I. Simulations of ionic currents and concentration changes. *Circ. Res.* 74:1071–1096.

Matsushita, T., M. Oyamada, K. Fujimoto, Y. Yasuda, S. Masuda, Y. Wada, T. Oka, and T. Takamatsu. 1999. Remodeling of cell-cell and cell-extracellular matrix interactions at the border zone of rat myocardial infarcts. *Circ. Res.* 85:1046–1055.

Meunier, J. M., N. A. Trayanova, and R. A. Gray. 1999. Sinusoidal stimulation of myocardial tissue: effects on single cells. *J. Cardiovasc. Electrophysiol.* 10:1619–1630.

Nilius, B. 1988. Calcium block of guinea-pig heart sodium channels with and without modification by the piperazinylindole DPI 201–106. *J. Physiol.* 399:537–558.

Noble, D., and R. B. Stein. 1966. The threshold conditions for initiation of action potentials by excitable cells. *J. Physiol.* 187:129–162.

Peters, N. S., J. Coromilas, N. J. Severs, and A. L. Wit. 1997. Disturbed connexin43 gap junction distribution correlates with the location of reentrant circuits in the epicardial border zone of healing canine infarcts that cause ventricular tachycardia. *Circulation.* 95:988–996.

Peters, R. W., and M. R. Gold. 2001. Implantable cardiac defibrillators. *Med. Clin. North Am.* 85:343–367 (xi.).

Pumir, A., G. Romey, and V. Krinsky. 1998. Deexcitation of cardiac cells. *Biophys. J.* 74:2850–2861.

Ranjan, R., N. Chiamvimonvat, N. V. Thakor, G. F. Tomaselli, and E. Marban. 1998. Mechanism of anode break stimulation in the heart. *Biophys. J.* 74:1850–1863.

Rodriguez, B., B. M. Tice, J. C. Eason, F. Aguel, J. M. Ferrero Jr., and N. Trayanova. 2004. Effect of acute global ischemia on the upper limit of vulnerability: a simulation study. *Am. J. Physiol. Heart Circ. Physiol.* 286:H2078–H2088.

Schaffer, P., H. Ahammer, W. MuLLEr, B. Koidl, and H. Windisch. 1994. Di-4-ANEPPS causes photodynamic damage to isolated cardiomyocytes. *Pflugers Arch.* 426:548–551.

Sharifov, O. F., R. E. Ideker, and V. G. Fast. 2004. High-resolution optical mapping of intramural virtual electrodes in porcine left ventricular wall. *Cardiovasc. Res.* 64:448–456.

Sharma, V., S. N. Lu, and L. Tung. 2002. Decomposition of field-induced transmembrane potential responses of single cardiac cells. *IEEE Trans. Biomed. Eng.* 49:1031–1037.

Sharma, V., and L. Tung. 1999. Transmembrane responses of single guinea pig myocyte to uniform electric field stimulus. *J. Cardiovasc. Electrophysiol.* 10:1296.

Sharma, V., and L. Tung. 2001. Theoretical and experimental study of sawtooth effect in isolated cardiac cell-pairs. *J. Cardiovasc. Electrophysiol.* 12:1164–1173.

Sharma, V., and L. Tung. 2002. Spatial heterogeneity of transmembrane potential responses of single guinea-pig cardiac cells during electric field stimulation. *J. Physiol.* 542:477–492.

Sobie, E. A., R. C. Susil, and L. Tung. 1997. A generalized activating function for predicting virtual electrodes in cardiac tissue. *Biophys. J.* 73:1410–1423.

Stone, B. A., M. Lieberman, and W. Krassowska. 1999. Field stimulation of isolated chick heart cells: comparison of experimental and theoretical activation thresholds. *J. Cardiovasc. Electrophysiol.* 10:92–107.

Susil, R. C., E. A. Sobie, and L. Tung. 1999. Separation between virtual sources modifies the response of cardiac tissue to field stimulation. *J. Cardiovasc. Electrophysiol.* 10:715–727.

Tung, L. 1995. Electroporation of cardiac cells. *Methods Mol. Biol.* 48:253–271.

Tung, L. 1996. Detrimental effects of electric fields on cardiac muscle. *Proc. IEEE.* 84:366–378.

Tung, L., and J. R. Borderies. 1992. Analysis of electric field stimulation of single cardiac muscle cells. *Biophys. J.* 63:371–386.

Tung, L., N. Sliz, and M. R. Mulligan. 1991. Influence of electrical axis of stimulation on excitation of cardiac muscle cells. *Circ. Res.* 69:722–730.

Watanabe, T., P. M. Rautaharju, and T. F. McDonald. 1985. Ventricular action potentials, ventricular extracellular potentials, and the ECG of guinea pig. *Circ. Res.* 57:362–373.

Windisch, H., H. Ahammer, P. Schaffer, W. MuLLEr, and D. Platzer. 1995. Optical multisite monitoring of cell excitation phenomena in isolated cardiomyocytes. *Pflugers Arch.* 430:508–518.

Yao, J. A., W. Hussain, P. Patel, N. S. Peters, P. A. Boyden, and A. L. Wit. 2003. Remodeling of gap junctional channel function in epicardial border zone of healing canine infarcts. *Circ. Res.* 92:437–443.